# Flammability of Hydrocarbon and Carbon Dioxide Mixtures

Gant S.E.*[1], Pursell M.R.[1], Lea C.J.[2], Fletcher J.[1], Rattigan W.[1], Thyer A.M.[3], Connolly S.[3]

[1] Health and Safety Laboratory, Harpur Hill, Buxton, SK17 9JN

[2] Lea CFD Associates Ltd, 12 Sheraton Way, Buxton, SK17 6FA

[3] Health and Safety Executive, Redgrave Court, Bootle, L20 7HS

* Corresponding author

Tel: +44 (0)1298 218134; Fax: +44 (0)1298 218840

E-mail address: simon.gant@hsl.gov.uk

## Research Highlights

- Explosion measurements are reported for methane, $CO_2$ and air mixtures.
- Ignition of jet releases of methane and $CO_2$ mixtures in air is examined.
- A new flammability model for free jets gives good agreement with previous data.
- Ignition probability in jets found to be sensitive to disturbances from wind.

## Keywords

Flammability, ignition, hydrocarbon, carbon dioxide, jets, confined explosions

## Abstract

The effect of carbon dioxide ($CO_2$) concentration on the ignition behaviour of hydrocarbon and $CO_2$ gas mixtures is examined in both jets and confined explosions. Results from explosion tests are presented using a 20 litre explosion sphere and an 8 m long section of 1.04 m diameter pipeline. Experiments to assess the flame stability and ignition probability in free-jets are reported for a range of different release velocities. An empirically-based flammability

factor model for free-jets is also presented and results are compared to ignition probability measurements previously reported in the literature and those resulting from the present tests.

The results help to understand how $CO_2$ changes the severity of fires and explosions resulting from hydrocarbon releases. They also demonstrate that it is possible to ignite gas mixtures when the mean concentration is outside the flammable range. This information may be useful for risk assessments of offshore platforms involved in carbon sequestration or enhanced oil recovery, or in assessing the hazards posed by poorly-inerted hydrocarbon processing plant.



# 1. Introduction

The next decade is likely to see a rapid increase in the transport offshore of $CO_2$ for enhanced oil recovery and its sequestration into depleted oil and gas fields. As a result, hydrocarbon gas streams may become increasingly contaminated by $CO_2$, and indeed, it may even sometimes be advantageous to mix the two streams to reduce the hazard posed by fires and explosions from unintended releases. In addition to this, ageing offshore installations are now being decommissioned or dismantled at an increasing rate. Dismantling of poorly-inerted former hydrocarbon processing plant has been known to cause fires and explosions resulting in fatalities. For these operations, risk assessments need to incorporate consequence modelling that takes into account the presence of $CO_2$, or other inert gases, and the new or modified hazards including changes in fire and explosion properties, and the risk of asphyxiation.

The effect of $CO_2$ and other inert gases on the flammability limits of static hydrocarbon mixtures has been studied extensively previously by, for example, Coward and Jones (1952), Zabetakis (1965), Beyler (1988) and Drysdale (1998). It is well known that the flammability

of mixtures is influenced by the experimental mode of investigation. Measurements of the flammability limits of premixed hydrocarbon and $CO_2$ gas mixtures in air have been reported by Kondo et al. (2006), using an explosion bomb similar to that described in ASTM (2009). It was found that the inert:fuel and feed ratio of 4:1 $CO_2$ to methane by volume was necessary to render a mixture inert, irrespective of the proportion of air present. This is equivalent to a $CO_2$ concentration of approximately 25% vol/vol in the methane-$CO_2$-air mixture when conditions are stoichiometric. Similar findings were previously reported by Coward and Jones (1952), based on tests involving upward flame propagation in a 10-inch diameter tube.

The flammability of non-premixed jet releases of hydrocarbon gases was investigated extensively at British Gas in the late 1970's and 1980's (Birch et al., 1978, 1979, 1981, 1989; Smith et al. 1986). In these studies, ignition probabilities were determined at various different locations within the jets by recording the proportion of successful ignitions following multiple ignition attempts. The ignition probability was found to be highest in regions where the concentrations were close to stoichiometric. On the centreline of the free jets, beyond the point where the mean gas concentration fell below half the Lower Flammability Limit (50% LFL), the ignition probability was found to fall essentially to zero. At the boundary of the jets, however, where the mean concentration was as low as 10% LFL, it was still found possible to ignite the mixture at times, due to turbulent fluctuations in the local fuel concentration.

More recently, the spark ignition of turbulent non-premixed jets has been examined by Ahmed and Mastorakos (2006) and Mastorakos (2009). They noted that high jet velocities reduced the ignition probability, due to convective heat loss from the spark in the early stages of the ignition process. Other factors affecting the likelihood of ignition included the spark position, spark width, ignition energy and local strain rate of the flow.

To examine how $CO_2$ changes the ignition behaviour of hydrocarbon gas releases, the present work considers both premixed and non-premixed mixtures of $CO_2$ and methane gas in air. For

the non-premixed gas jets, the ignition probability is assessed following a similar approach to that taken by Birch et al. (1981, 1988) and Smith et al. (1986). An empirically-derived jet flammability model is also presented. Its performance is first validated using the experiments of Smith et al. (1986), and then the model predictions are compared to the measurements of the present work. Finally, conclusions are presented and suggestions provided for future work. The Appendix gives full mathematical details of the flammability model.

# 2. Experiments

## 2.1. Measurement Techniques

### 2.1.1 Explosion Tests

A series of small-scale explosion experiments were carried out to determine the explosion behaviour of mixtures of methane with $CO_2$ and air. The tests were performed in a temperature controlled (25 °C) standard 20 litre explosion sphere in accordance with British Standard, BS EN 1839 (BSI, 2004). The quantities of each substance were measured by partial pressure readings using a high precision digital pressure gauge. Ignition was effected by a 10 kV spark generator across two stainless steel electrode tips, and the explosion overpressures were recorded using two calibrated Kistler (type 701A) pressure transducers, with a data sampling rate of 50 kHz. In each test, the methane concentration was 10% vol/vol and the $CO_2$ concentration was varied between 0% and 20% vol/vol, with the remainder being air.

Larger gas explosions were conducted at HSL in a facility designed to test the explosion resistance of passive fire protection materials. The apparatus consisted of a number of 1.04 m internal diameter steel pipe sections as shown in Figure 1. The total length was 8 m, giving a volume of 6.8 $m^2$. The gas was ignited at one end of the pipe and the explosion was allowed

to propagate along the pipe and exit at the opposite open end, where the flow was incident on a nearby 1 $m^2$ test piece. The overpressure of the explosion exiting the pipe end could be controlled by varying the coverage of the top vent, which for all tests reported here was set with three quadrants open (see Figure 1b). Methane and $CO_2$ were introduced into the vessel from remotely controlled gas bottles. Polythene sheets were placed over the top vent and the open end to retain the gas during filling, and the contents of the pipe were mixed using an electrically driven fan. Ignition was effected using a 5 grain blackpowder fuse and the gas concentration was monitored using a GA 94A Landfill Gas Analyser (Geotechnical Instruments). The target methane concentration was the stoichiometric value for methane in air, i.e. 9.5% vol/vol. However, due to the response time of the gas analyser, the final gas concentrations varied from the target by a small margin. Four tests were performed with $CO_2$ concentrations of 0%, 3.7%, 7% and 12% vol/vol and corresponding methane concentrations of 9.3%, 9.4%, 10.5% and 8.2% vol/vol, with the remainder being air. The overpressures generated by the explosions were monitored using four pressure transducers (model: ETS-IA-375, Kulite Semiconductor Products); one close to the ignition point, another near the open end, and two mounted in the test plate (as shown in Figure 1c). Data was logged using a high-speed data logger (DewiSoft v7.0) at a sampling rate of 50 kHz.

### 2.1.2 Jet Ignition Tests

Two sets of jet ignition tests were performed in the present work. The first consisted of bulk ignition tests, where the gas jet was ignited using a propane blow torch and the resulting stability of the flame was categorised. Flame lift-off distances were measured from video recordings of the experiments. The second set of tests involved ignition probability measurements, where ignition of the gas jet was attempted using a spark-ignition system, and the number of successful ignitions was recorded. Both sets of tests used the same gas release apparatus. Methane and $CO_2$ gases were provided from gas cylinders regulated to 3 bar. Individual gas flowrates were controlled via adjustable rotameters and combined at a T-

junction before being delivered to the release pipe via 5 metres of fire resistant gas tubing. The release pipe, which had an inner diameter of 6 mm and length of 400 mm, was clamped to a metal frame such that the gas was released vertically upwards. The experiments were performed in a sheltered courtyard that was walled on four sides and open to the atmosphere. This allowed experiments to be performed in moderate weather conditions, but tests could only be performed in low to moderate wind speeds since higher wind speeds clearly affected the gas jet dispersion behaviour.

The bulk ignition characteristics were examined at 3 different total flowrates (30 l/min, 50 l/min and 90 l/min), details of the corresponding exit velocities and Reynolds numbers are given in Table 1. The ignition response was categorised in a similar manner to the approach taken by Thyer et al. (2009) – see Table 2. For Classes 1, 2, and 3 the blowtorch flame was kept in the gas jet, whereas for Classes 4 and 5 the flame was removed as soon as ignition occurred. Each test was recorded using a video camera (HDC-SD10, Panasonic) at a frame rate of 25 fps. Individual images were captured and processed using HD Writer AE v1.5 (Panasonic) and VirtualDub. Flame lift-off distances were determined during stable periods of combustion where wind effects were minimal (i.e. the flame was vertical). The image analysis software ImageJ was used to identify the position of the flame front and measure the distance from the release point. Since the lift-off distance varied over time, the reported values were determined from a minimum of 500 frames, and the standard deviation in flame height was found to be ±18%.

Ignition probability measurements were performed using a spark ignition system, which comprised a variable high voltage power source, two 1 GOhm resistors, a 2 nF capacitor, high tension wires and tungsten electrodes (diameter = 2 mm, length = 150 mm). The power source allowed the capacitor to be charged to 15 kV, and the system produced a spark every four seconds. The tungsten electrodes were positioned in the gas jet with a separation distance of 2 mm. Ignition tests were performed in batches, with the gas shut off for a period of 20 to 30

seconds between each batch to avoid build up of combustible gases, or to allow venting of combustion products when ignition had occurred. Each batch consisted of a maximum of ten sparks. However, when ignition occurred the batch was terminated. For each ignition location, a total of 100 batches were performed. In many cases, ignition occurred before the maximum of ten ignition attempts had been reached. On average, 250 ignition attempts were performed at each location. Tests were performed using either pure methane or a feed mixture comprising 80% vol/vol methane and 20% vol/vol $CO_2$, at a flowrate of 90 l/min (corresponding to an exit velocity of 53.1 m/s, and a Reynolds number of 19,359, for pure methane). This condition was chosen so as to be comparable with the previous work of Birch et al. (1981) and Smith et al. (1986) who used Reynolds Numbers of between 12,500 and 22,000.

The mean gas concentrations of methane and $CO_2$ in the unignited gas jet were determined at the same positions where the ignition probability was measured, using a GA 2000 Portable Gas Analyser (Geotechnical Instruments). The accuracy of the analyser was ±0.5% over the range 0% to 15% vol/vol, ±1.0% over the range 15% to 30% vol/vol, and ±3.0% over the range 30% to 100% vol/vol. Gases were sampled via a 4 mm inner diameter stainless steel tube that was positioned in the gas jet. The reported values are the average of 60 readings taken at 1 s intervals. The standard deviation of the measurements was ±0.8% vol/vol for methane and ±0.1% vol/vol for $CO_2$.

## 2.2. Experimental Results

To allow a direct comparison between the air premixed explosion tests and the non-premixed jet ignition tests, results are presented in terms of a notional ‘feed’ gas in the absence of any air, i.e. the $CO_2$ feed concentration is the ratio of the $CO_2$ volume to the total volume of $CO_2$ and methane.

### 2.2.1 Bulk Ignition Characteristics

The bulk ignition tests examined the response of the $CO_2$-methane jet to pilot ignition from a propane blow torch. Three different exit velocities were studied, with $CO_2$ feed concentrations of up to 70% vol/vol. The behaviour of the system was classified according to the ignition response class defined in Table 2. The change in the ignition response class in response to $CO_2$ addition is shown in Figure 2. At all gas velocities, the severity of the ignition response decreased with increasing $CO_2$ concentration, as expected. At gas velocities of 29.5 m/s and 17.7 m/s the methane was completely inert with $CO_2$ concentrations in the region of 60% to 70% vol/vol in the feed gas. Due to the limited range of the gas flow meters, it was not possible to test $CO_2$ concentrations greater than 45% vol/vol at the highest gas velocity of 53.1 m/s. However, it is expected that it would follow a similar trend to the other two conditions, and be completely inert with a $CO_2$ concentration of around 60% vol/vol in the feed gas. For the lower velocity gas jets, a higher ignition class was maintained over a wider range of $CO_2$ concentration. This behaviour is consistent with the lower flame speed maintaining a stable flame in these cases. The observed change in ignition class with $CO_2$ concentration demonstrates that in situations where jet light-up cannot be sustained over a long period, there can still be sufficient methane and air to promote combustion. Thus if a partially inerted mixture was released onto a continuous ignition source, such as an on-going hydrocarbon fire, it could add to the severity of the fire.

For the two higher gas velocities (29.5 m/s and 53.1 m/s), the pure methane flame was not attached to the release pipe but was observed at a stable location downstream from the release point, where the advancing gas velocity matched the flame speed. The location of the lift-off distance for these two releases is shown in Table 3. The distance from the pipe orifice to the flame front at the higher velocity of 53.1 m/s was roughly twice that achieved with the lower velocity of 29.5 m/s. The local flow velocity at these positions, determined from an empirical jet model (see Appendix), shows that the velocity at the flame front location in the two tests

was similar, falling within the region of 9.2 ± 0.4 m/s. Analysis of the flame lift-off position was also undertaken for the tests involving $CO_2$-methane mixtures where a stable flame was observed (Classes 4 and 5 in Figure 2). The results are presented in Figure 3 for the two highest gas flowrates (29.5 m/s and 53.1m/s). At the lower gas velocity of 17.7m/s, the flame was not sufficiently stable to provide reliable measurements. For release velocities of both 29.5 m/s and 53.1m/s, the flame front moved further downstream with increasing $CO_2$ concentration. At 29.5 m/s the flame front lift distances were 6.9 cm, 10.8 cm and 17.3 cm for $CO_2$ concentrations of 0%, 10% and 20% respectively; and at 53.1 m/s the distances were 12.8 cm, 15.3 cm and 16.1 cm for $CO_2$ concentration of 0%, 6% and 11%. These positions translate into the reduced flame front speed, as shown in Figure 3. Over the limited range considered, the relationship between the flame front speed and $CO_2$ concentration was linear, however a number of factors will dictate the location of the stable flame front, including the local gas velocity, the local gas composition, the chemistry of the combustion reaction and the effect of the inert gas on this reaction rate and its effect on the flammable limits of the gas mixture.

### 2.2.2 Explosion Tests

The results of the explosions tests in the 20 litre explosion sphere and the 1 m diameter pipeline are shown in Figure 4. The two sets of overpressure measurements are normalised using the maximum pressures obtained from the experiments with pure methane, which were 7.4 bar and 0.72 bar in the 20 litre sphere and pipeline tests, respectively. Higher pressures were obtained in the explosion sphere as it was fully enclosed, whereas the pipeline was open at one end and had additional vents. For both configurations it was found that increasing the $CO_2$ concentration caused a decrease in the maximum overpressure ($P_{max}$), with the effect being more pronounced in the 1 m diameter pipeline. The rate of change of pressure was also greatly reduced in all of the tests where $CO_2$ was present; indicating that the flame front speed was reduced (for details of these results, see Pursell et al., 2011). In the 20 litre explosion

vessel, ignition was detected at a $CO_2$ feed concentration of 60% vol/vol, but not at 63% vol/vol. However, in the 1 m diameter pipeline tests no ignition was detected at 59% vol/vol. This discrepancy between the results obtained from the two sets of apparatus is likely to have been due to inhomogeneities in gas concentration that could occur in the larger pipe, where mixing was effected by internal gas circulation driven by a fan blade.

The results from the 20 litre sphere agree well with the previous findings of Kondo et al. (2006). For the same proportions of methane and air, Kondo et al. (2006) found an inerting $CO_2$ feed concentration of approximately 61 % vol/vol. This demonstrates that under well-defined and controllable conditions in explosion spheres, comparable results can be obtained. However, the variation between the present results obtained from two quite different experimental setups highlights the potential uncertainty that can exist when identifying the correct inerting concentration for different geometries and scenarios where uncertain degrees of mixing and turbulence may be present. Kondo et al. (2006) studied a wider range of methane and air concentrations than was considered in the present work. They found that the maximum $CO_2$ feed concentration that was necessary to suppress ignition completely was 79.4% vol/vol, for a mixture in which the ratio of methane to the total volume (methane plus $CO_2$ and air) was 6.5% vol/vol.

Comparing the ignition behaviour observed in the premixed ignition tests to that obtained from the bulk ignition tests of pressurised jet releases it is seen that the levels of $CO_2$ required to render the jet completely inert were below the values reported by Kondo et al (2006), who found in static gas mixtures that a concentration of 79.4% vol/vol $CO_2$ was necessary to inert the mixture. The trends shown in Figure 2 indicate that for gas jets, the release velocity provides an additional inhibiting factor for ignition and stable flame formation. Standard static tests of flammability, such as a 20 litre explosion sphere, may therefore be considered to provide conservative estimates of the $CO_2$ concentration required to inert the mixture during unintended releases from pressurised sources.

# 3. Jet Flammability Model

## 3.1. Theoretical Basis

To be able to predict the probability of ignition at any point in the flow, it is necessary to know the fraction of time that a source of ignition encounters gas concentrations between the upper and lower flammability limits. This quantity, i.e. the fraction of time that the gas mixture is flammable, is termed the 'Flammability Factor', $F$ (Birch et al., 1981). It can be determined by integrating the Probability Density Function (PDF) of concentration at the ignition location, $p(\tilde{c})$, between the flammability limits, as follows:

$$F = \int_{c_L}^{c_U} p(\tilde{c}) d\tilde{c} \qquad (1)$$

where $c_U$ and $c_L$ are the static upper and lower flammability limits, respectively. The tilde symbol is used here to signify the time-varying instantaneous concentration at any point in space.

It was demonstrated by Birch et al. (1981) that the flammability factor determined from Equation (1) provides good predictions of the measured ignition probability for gas releases in air at ambient temperatures. Flammability factors have also been computed and compared to measurements of ignition probability for methane and propane jets by Smith et al. (1986) and recently for hydrogen jets by Schefer et al. (2010). In both of these studies, it was demonstrated that there was good agreement between the predicted flammability factor and the measured ignition probability.

In the present work, the shape of the concentration PDF is specified as a function of the mean and Root-Mean-Square (RMS) concentration, and the turbulence intermittency. For free jets,

the values of these parameters are found from empirical formulae taken from the literature, as follows:

- The mean velocity and mean concentration along the centreline of the subsonic jet are determined from empirical profiles from Chen and Rodi (1980), with some minor changes to the model constants to achieve smooth transitions between momentum-dominated and intermediate regions in the jet (see Appendix);
- In the radial direction, Gaussian profiles are assumed for the mean velocity and mean concentration, using spreading rates given by Chen and Rodi (1980) and Birch et al. (1978);
- The RMS concentration fluctuation is determined using the $\alpha$-$\beta$ model of Chatwin and Sullivan (1990);
- The turbulent intermittency in the jet is determined using the empirical model of Kent and Bilger (1976);
- The shape of the PDF is assumed to comprise the sum of a delta function and a truncated Gaussian, using conditionally sampled mean and RMS values, based on the model of Birch et al. (1981);
- The two-part PDF is integrated using error functions between upper and lower flammability limits, which are calculated for the methane and $CO_2$ mixtures using a modified Le Chatelier's law developed by Kondo et al. (2006).

The model has many similarities to that presented by Birch et al. (1981), except that they did not describe the profiles used for intermittency, and mean and RMS concentration, which were instead probably taken from unpublished experimental measurements (personal communication M. Fairweather, March 2010). For background information on the development of the present model, see Gant et al. (2011a, 2011b).

Following ignition at a point in a gas jet, a flame kernel may be convected downstream and eventually be extinguished, or alternatively it may grow both downstream and upstream to light-up the whole jet. The probability that light-up occurs, rather than just a localised ignition, can be very different (Birch et al., 1981, Smith et al., 1986). Localised ignition only requires instantaneous gas concentrations to be within the flammability limits and for there to be present an ignition source of sufficient energy. Light-up of the whole jet depends on other factors, such as the existence of a pathway for the flame to propagate from one flammable region to another, and for the local flame speed to exceed local flow speeds.

The flammability factor predicts the probability of only a flame kernel being produced. Subsequently, this kernel may or may not lead to light-up of the jet. The concept of the flammability factor is therefore consistent with the philosophy commonly used in risk assessments, where a source of ignition in the presence of a flammable mixture is assumed to pose a hazard, and it is not required to demonstrate the presence of a flammable pathway back to the source (see also Webber, 2003). In principle, it is possible to predict jet light-up using Computational Fluid Dynamics (CFD) methods based on Large Eddy Simulation (LES), as shown by Triantafyllidis et al. (2009), but it requires significant computing resources.

High-pressure gas release experiments performed by Birch et al. (1988), where the flow was sonic at the source, showed that the flammability factor is also a valid indicator of ignition probability for high-speed releases, once the jet has decelerated to sub-sonic flow. Birch et al. (1989) also later investigated the ignition behaviour of jets in a cross-flow.

The addition of carbon dioxide, nitrogen or any other inert gas to a fuel does not affect the validity of the flammability factor concept for predicting ignition probability. The same physics applies and all that is required is to modify the upper and lower flammability limits for the particular gas mixture.

Similarly, the flammability factor should provide good predictions of the ignition probability at elevated temperatures, provided that suitable corrections are employed to the static flammability limits (see, for example, Drysdale, 1998). This may need to be considered in assessing Major Accident Hazard (MAH) scenarios in which an existing fire has increased ambient temperatures. Due to the wider flammability limits at higher temperatures, the size of the region where the jet is ignitable is likely to increase and the model presented here may provide non-conservative predictions of the hazard range. Additional complications may be introduced by the need to account for changes in local temperatures as the jet of hot gas mixes with cooler ambient air, and the presence of any combustion products from the existing fire. The situation will also clearly become more complex as temperatures approach the auto-ignition temperature.

## 3.2. Model Validation

To validate the new model for the flammability factor of subsonic free jets, it has been used to reproduce the results of Smith et al. (1986). Predictions of the mean gas concentration and flammability factor along the centreline of free jets are presented in Figure 5 for a natural gas jet with a release velocity of 50 m/s and orifice diameter of 6.35 mm. Smith et al. (1986) assumed that the virtual source of the gas jet was located four diameters upstream of the orifice. The same offset is used in the present model results, and the results are given in Figure 5 with the axial displacement measured from the virtual jet origin rather than the orifice.

The flammability factor predicted by the present model shows some small differences compared to the previous results of Smith et al. (1986). In the far field, where mean concentrations fall below the LFL, the new model predicts the flammability factor to decay

more rapidly to zero than the model of Smith et al. (1986). The results are therefore in slightly better agreement here with the experiments. In the near-field of the jet, where fuel concentrations are above the Upper Flammability Limit (UFL), the new model predicts higher flammability factors than were obtained by Smith et al. (1986), in slightly worse agreement with the experiments. These differences are fairly minor, however, and overall the predicted flammability factor is in good agreement with the measured ignition probabilities and previous model predictions.

Additional comparisons of the model's performance against the predictions and measurements of Smith et al. (1986) and Birch et al. (1981) are given by Gant et al. (2011b). Overall, these comparisons show a similar level of agreement to that shown in Figure 5. The results of this short study indicate that the model provides reliable predictions of the flammability factor for sub-sonic free jets in a quiescent environment.

## 3.3. Results and Discussion

The measured probability of ignition is compared to the predicted flammability factor for pure methane and the mixture of 80% vol/vol methane and 20% vol/vol $CO_2$, in Figure 6. The upper and lower flammability limits shown in these graphs are 15% and 5% for pure methane, and 13.4% and 5.1% for the methane-$CO_2$ mixture, as determined by the model of Kondo et al. (2006). The measured ignition probabilities are shown with error bars representing the statistical uncertainty associated with one standard deviation, using the same approach taken by Birch et al. (1981).

Both the measurements and the model predictions show that the presence of 20% vol/vol $CO_2$ in the source gas reduces the axial extent of the flammable region. The model predicts the distance from the source to a flammability factor of 50% to decrease by around 11%, from

74 cm to 66 cm as the $CO_2$ concentration increases from 0% to 20% vol/vol. On the centreline of the jet at a distance of 20 cm from the nozzle, the model predicts the mean concentration to be above the UFL. However, in the experiments, it was found possible to ignite the jet at this location, due to concentrations fluctuating within the flammable range, as predicted by the flammability factor model.

There is reasonable agreement between the measured and predicted ignition probabilities up to a distance of around 30 cm from the nozzle. However, further downstream, the model produces significantly higher values than were measured experimentally. The measurements found practically zero ignition probability at distances more than 70 cm and 50 cm for the pure methane and methane-$CO_2$ jets, respectively, whilst the model predicted the jet to be ignitable up to a distance of 100 cm downstream from the source in both cases.

The ignition probability data along the centreline of the jet are plotted against the mean concentration, instead of the axial displacement, in Figure 7. Plotting the data in this way accounts for any discrepancies between the predicted and measured mean concentration. Figure 7 shows that the measured ignition probabilities span a similar range of mean concentration to that predicted by the model. However, the measured ignition probabilities remain much lower than those predicted by the empirical model. All of the measured ignition probabilities are less than 60% whereas they are predicted to reach nearly 100% in places.

One of the possible explanations for the low ignition probability measured in the experiments is that not all of the ignitions were detected. Very small pockets of gas could have been ignited that were too small to be visible. In the experiments, ignitions were detected either audibly or visibly. In those cases where bright sunshine partially obscured the directly visible flame, its presence was detected by the shadow produced on an adjacent wall, from the Schlieren effect. A similar approach appears to have been taken by Birch et al. (1981) who described ignitions as simply being “observed” in their experiments. In the more recent work

of Schefer et al. (2010), thermocouples downstream of the ignition location were used to determine the presence of a flame kernel.

Even if some ignitions were not detected in the present experiments, this is not considered to offer a plausible explanation for the discrepancy of 40% between the measured ignition probability and predicted flammability factor. It is considered more likely that the differences arose from gusts of wind that disturbed the jet and led to gas concentrations varying more over time. The test area used in the experiments was open to the atmosphere and although tests were conducted in low to moderate wind speeds to minimise its effect, some disturbances probably still occurred. These would have been more significant in the far-field of the jet, where its momentum was low. Beyond a distance of 30 cm, the maximum velocity on the centreline of the jet was predicted to fall below 5 m/s. Although the results presented in Figure 7 accounts for the reduction in mean gas concentration due to these disturbances, the turbulent fluctuations in the jet will also have been affected. The same mean gas concentration can be produced by varying the gas concentration between wider limits, which could reduce the proportion of time the mixture spends within the flammable range, hence lowering its likelihood of ignition.

In realistic release conditions, following a failure on an offshore platform for example, it is unlikely that the flow around the release point will be quiescent (see Saunders and Ivings, 2005). The results presented here are useful in demonstrating that even relatively small gusts of wind may have a significant effect on the dispersion of the gas and its chances of igniting in such cases. The model predicted higher ignition probabilities along the axis of the jet than were measured in the present experiments, i.e. the model results were conservative in terms of the predicted hazard. However, without further analysis it is unclear whether the model will always return conservative values, or whether under certain conditions, such as a co-flowing wind, turbulent fluctuations could be suppressed, leading to higher ignition probabilities.

Contours of the predicted flammability factor for the pure methane and methane-$CO_2$ jets, are shown in Figure 8. The position of the mean predicted LFL and UFL, based on the predicted mean gas concentration, are indicated by bold red lines, and symbols show the locations where the ignition probability was measured in the experiments. The results show that the addition of $CO_2$ decreases the area over which the gas mixture can be ignited, by decreasing both its axial and radial extent. Where the mean gas concentration is at the LFL or UFL, the predicted flammability factor is around 50%, in agreement with the previous findings of Smith et al. (1986).

The flammability factor model presented here is based on empirically-derived correlations and is valid only for free-jets in a quiescent atmosphere. The feasibility of using CFD to extend predictions of the flammability factor beyond such simple flows was examined in detail by Gant et al. (2011b). Previous work in this field, such as that by Alvani and Fairweather (2008), was reviewed and a simplified methodology was proposed which retains many of the benefits of more sophisticated approaches.

# 4. Conclusions

The effect of $CO_2$ on the ignition of both premixed and non-premixed fuel-air mixtures has been investigated. Increasing the concentration of $CO_2$ was shown to reduce the overpressure obtained in explosion tests. In well-controlled small-scale explosions involving mixtures of methane, $CO_2$ and air, the gas mixture was found to be inerted at a $CO_2$ feed concentration of 63% vol/vol. This finding was in good agreement with flammability limits reported previously by Kondo et al. (2006). In larger-scale methane explosion tests, ignition did not occur at a $CO_2$ feed concentration of 59%. The observed differences between the two test scenarios were considered most likely to have resulted from imperfect mixing of the gases prior to ignition.

Investigations of the bulk ignition behaviour of jet releases of methane and $CO_2$ mixtures showed that stable combustion was possible with $CO_2$ concentrations in the source gas up to 33% vol/vol. At higher $CO_2$ concentrations up to around 60% to 70% vol/vol in the source gas, a stable flame could not be sustained, but intermittent flames could still be produced and the presence of the gas mixture increased the flame length of a pilot flame. Complete inerting was only achieved at higher $CO_2$ concentrations. The stability of the flame was also affected by the fuel gas exit velocity. These findings are in agreement with flammability limits published previously in the literature, which suggest that a concentration of 80% $CO_2$ in the source gas is necessary to render the jet completely inert. In relation to process safety, the results show that care should be taken when inerting hydrocarbons lines unless $CO_2$ concentrations are at a sufficiently high level (for methane, around 80% vol/vol $CO_2$), as releases may otherwise result in combustible mixtures forming as the gas dilutes in air. If a partially inerted mixture is released onto a continuous ignition source, such as an on-going hydrocarbon fire, it could add to the severity of the fire.

A new empirically-based model for the ignition probability of free jets has been presented and validated against the previously published work of Smith et al. (1986). It has then been applied to study jets of pure methane and a methane-$CO_2$ mixture, for which new experimental data has also been presented. The results showed that the ignitable region in a jet of methane containing 20% $CO_2$ by volume was smaller than that in the equivalent pure methane release, as expected. The results also demonstrated that it is possible to ignite gas jets at points in the flow where the mean concentration was outside the static flammability limits. The agreement between the model predictions and the measured ignition probability were good in the near-field but were found to deteriorate at a distance of around 30 cm downstream from the orifice. Generally the model predictions were significantly higher than those measured. These differences were attributed to the effect of the wind in the experiments.

The flammability factor model presented here can easily be extended to consider other gas mixtures. Applications include discharges from storage tanks with nitrogen-inerting systems, and hydrogen and inert gas mixtures used in pre-combustion $CO_2$-capture power stations. The same fundamental principles of the flammability factor can also be used to analyse the toxic load a person may receive from atmospheric exposure to fluctuating concentrations of a toxic gas, aerosol or dust.

## Disclaimer

This publication and the work it describes were funded by the Health and Safety Executive (HSE). Its contents, including any opinions and/or conclusions expressed, are those of the authors alone and do not necessarily reflect HSE policy.

## Acknowledgements

The authors would like to thank Dr. Adrian Kelsey (Health and Safety Laboratory) and Professor Mike Fairweather (Leeds University) for help in this work.

## References

Ahmed, S.F., Mastorakos, E., 2006. Spark ignition of lifted turbulent jet flames. Combustion and Flame 146, 215-231.

Alvani, R.F., Fairweather, M., 2008. Prediction of the ignition characteristics of flammable jets using intermittency-based turbulence models and a prescribed PDF approach. Computers and Chemical Engineering 32, 371-381.

ASTM (2009) Standard test method for concentration limits of flammability of chemicals (vapors and gases), ASTM E681 - 09, ASTM International, West Conshohocken, Pennsylvania, USA.

Beyler, C., 1988. Flammability limits of premixed and diffusion flames, in: SFPE Handbook of Fire Protection Engineering, Society of Fire Protection Engineers, Bethesda, Maryland, USA.

Birch, A.D., Brown, D.R., Dodson, M.G., Thomas, J.R., 1978. The turbulent concentration field of a methane jet. J. Fluid Mech. 88, 431-449.

Birch, A.D., Brown, D.R., Dodson, M.G., Thomas, J.R., 1979. Studies of flammability in turbulent flows using laser Raman spectroscopy. 17th Symposium (International) on Combustion, The Combustion Institute, pp.301-314.

Birch, A.D., Brown, D.R., Dodson, M.G., 1981. Ignition probabilities in turbulent mixing flows. 18th Symposium (International) on Combustion, The Combustion Institute, pp.1775-1780.

Birch, A.D., Brown, D.R., Cook, D.K., Hargrave, G.K., 1988. Flame stability in under-expanded natural gas jets. Combust. Sci. and Tech. 58, 267-280.

Birch, A.D., Brown, D.R., Fairweather, M., Hargrave, G.K., 1989. An experimental study of a turbulent natural gas jet in a cross-flow. Combust. Sci. and Tech., 66, 217-232.

BSI (2004) Determination of explosion limits of gases and vapours. BS EN 1839:2003, The British Standards Institution (BSI), London, UK.

Chatwin, P.C., Sullivan, P.J., 1990. A simple and unifying physical interpretation of scalar fluctuation measurements from many turbulent shear flows. J. Fluid Mech. 212, 533-556.

Chen, C.J., Rodi, W., 1980. Vertical turbulent buoyant jets: a review of experimental data. Pergamon Press.

Coward, H.F., Jones, G.W., 1952. Limits of flammability of gases and vapors. Bulletin 503, Bureau of Mines, U.S. Government Printing Office.

Drysdale, D. 1998 An introduction to fire dynamics, second ed. Wiley, Chichester, UK.

Gant, S.E., Pursell, M.R., Lea, C.J., Thyer, A.M., Connolly, S., 2011a. Flammability of hydrocarbon/$CO_2$ mixtures: Part 2. Predictive models for gas jet ignition. Accepted for Publication, Proc. IChemE Hazards XXII Conference, Liverpool, UK, 11-14 April 2011.

Gant, S.E., Lea, C.J, Pursell, M., Rattigan, W., Thyer, A., 2011b. Flammability of hydrocarbon and carbon dioxide mixtures: experiments and modelling. HSL Report MSU/2010/21, Available from Health and Safety Laboratory, Buxton, UK.

Kent, J.H., Bilger, R.W., 1976. The prediction of turbulent diffusion flame fields and nitric oxide formation. 16th Symposium (International) on Combustion, The Combustion Institute, pp.1643-1656.

Kondo, S., Takizawa, K., Takahashi, A., Tokuhashi, K., 2006. Extended Le Chatelier's formula for carbon dioxide dilution effect on flammability limits. J. Hazardous Mater. A138, 1-8.

Mastorakos, E., 2009. Ignition of turbulent non-premixed flames. Progr. Energy Combust. Sci. 35, 57-97.

Pursell, M.R., Gant, S.E., Fletcher, J., Rattigan, W., Thyer, A.M., Connolly, S., 2011. Flammability of hydrocarbon/$CO_2$ mixtures: Part 1. Ignition and explosion characteristics. Accepted for Publication, Proc. IChemE Hazards XXII Conference, Liverpool, UK, 11-14 April 2011.

Saunders, C.J., Ivings, M.J., 2005. Natural ventilation of offshore modules, HSE Research Report RR402, Health and Safety Executive, Sudbury: HSE Books (http://www.hse.gov.uk/research/rrpdf/rr402.pdf, accessed February 2011).

Schefer, R.W., Evans, G.H., Zhang, J., Ruggles, A.J., Greif, R., 2010. Ignitability limits for combustion of unintended hydrogen releases: experimental and theoretical results. Int. J. Hydrogen Energy, Article in Press, doi:10.1016/j.ijhydene.2010.04.004.

Smith, M.T.E., Birch, A.D., Brown, D.R., Fairweather, M., 1986. Studies of ignition and flame propagation in turbulent jets of natural gas, propane and a gas with a high hydrogen content. 21st Symposium (International) on Combustion, The Combustion Institute, pp.1403-1408.

Thyer, A. M., Kay, J., Gant, S. E., 2009. Investigations into the flammability of propane/carbon dioxide, hydrogen/carbon dioxide and hydrogen/nitrogen mixtures. Proc. IChemE Hazards XXI Conference, Manchester, UK, 9-12 November 2009, Rugby: IChemE, ISBN: 9780852955369.

Triantafyllidis, A., Mastorakos, E., Eggels, R.L.G.M., 2009. Large eddy simulation of forced ignition of a non-premixed bluff-body methane flame with conditional moment closure. Combust. Flame 156, 2328-2345.

Webber, D.M., 2003. On defining a safety criterion for flammable clouds. HSL Report CM/02/15, Available from Health and Safety Laboratory, Buxton, UK.

Zabetakis, M.G. 1965. Flammability characteristics of combustible gases and vapors. Bulletin 627, Bureau of Mines, U.S. Government Printing Office.

# 5. Appendix: Flammability Factor Model Details

The mean velocity and concentration profiles along the centreline of the jet, developed by Chen and Rodi (1980), consist of two equations which are valid in separate regions of the flow: the momentum-dominated region near the jet orifice and an intermediate region further downstream where inertial forces are weaker and buoyancy forces start to become important. The boundary between these two regions is defined using a dimensionless axial distance, $x^*$:

$$x^* = Fr^{-1/2}\left(\frac{\rho_0}{\rho_a}\right)^{-1/4}\left(\frac{x'}{D}\right) \tag{2}$$

where $x'$ is the axial distance from the virtual origin of the jet (see Chen and Rodi, 1980), $D$ is the orifice diameter, $\rho$ the density and subscripts "$a$" and "0" refer to ambient and jet orifice values respectively. The Froude number, $Fr$, is given by:

$$Fr = \frac{U_0^2}{gD(\rho_a - \rho_0)/\rho_0} \tag{3}$$

where $U_0$ is the velocity at the jet orifice and $g$ is the acceleration due to gravity. In the momentum-dominated region near the jet, where $x^* < 0.5$, the mean centreline velocity, $U_{cl}$, and centreline concentration, $C_{cl}$, are given by:

$$U_{cl} = 6.2U_0\left(\frac{\rho_0}{\rho_a}\right)^{1/2}\left(\frac{x'}{D}\right)^{-1} \tag{4}$$

$$C_{cl} = 5C_0\left(\frac{\rho_0}{\rho_a}\right)^{-1/2}\left(\frac{x'}{D}\right)^{-1} \tag{5}$$

whilst in the intermediate region, where $x^*$ is between 0.5 and 5.0, they are given by:

$$U_{cl} = a_U U_0 Fr^{-1/10}\left(\frac{\rho_0}{\rho_a}\right)^{9/20}\left(\frac{x'}{D}\right)^{-4/5} \tag{6}$$

$$C_{cl} = a_C C_0 Fr^{1/8}\left(\frac{\rho_0}{\rho_a}\right)^{-7/16}\left(\frac{x'}{D}\right)^{-5/4} \tag{7}$$

Beyond the intermediate region, where $x^*$ is greater than 5.0, buoyancy forces become dominant and the flow exhibits plume-like behaviour. However, since the fluctuating gas concentrations in this region of the flow are below the LFL, it is only necessary here to consider the momentum-dominated and intermediate regions.

Values of 7.1 and 4.2 are taken for the constants $a_U$ and $a_C$ in Equations (6) and (7), respectively. These differ slightly from the values given by Chen and Rodi (1980) and Smith et al. (1986) who used, respectively, $a_U = 7.26$ and $a_C = 0.44$, and $a_C = 4.4$. The values have been chosen in the present study to produce smooth transitions in velocity and concentration between the momentum-dominated and intermediate regions. In the radial direction, the mean velocity and mean concentration are approximated using Gaussian profiles:

$$\frac{U}{U_{cl}} = \exp\left[-K_U\left(\frac{r}{x'}\right)^2\right] \tag{8}$$

$$\frac{C}{C_{cl}} = \exp\left[-K_C\left(\frac{r}{x'}\right)^2\right] \tag{9}$$

where constants $K_U$ and $K_C$ are given values 94.0 and 73.6, based on values given by Chen and Rodi (1980) and Birch et al. (1978), respectively. The RMS concentration is determined using the $\alpha$-$\beta$ model of Chatwin and Sullivan (1990):

$$\overline{c^2} = \beta C\left(\alpha C_{cl} - C\right) \tag{10}$$

where constants $\alpha$ and $\beta$ are given values of 1.27 and 0.14, respectively, based on Chatwin and Sullivan's (1990) analysis of the methane jet experiments of Birch et al. (1978). The turbulent intermittency, $I$, is calculated using the empirical formula of Kent and Bilger (1976):

$$I = \frac{K+1}{\left[\left(\frac{\overline{c^2}}{C^2}\right)+1\right]} \tag{11}$$

where $K$ is a constant given a value of 0.25 by Kent and Bilger (1976). To account for the change in shape of the concentration PDF with radius, the present model adopts the two-part PDF proposed by Birch et al. (1981) which smoothly varies between a truncated Gaussian distribution and a delta-function, based on the intermittency:

$$p(\widetilde{c}) = \underbrace{(1-I)\delta(\widetilde{c})}_{} + \frac{IA}{\sqrt{2\pi\overline{c_c^2}}}\exp\left[-\frac{(\widetilde{c}-C_c)^2}{2\overline{c_c^2}}\right] \tag{12}$$

where the subscript '$c$' denotes conditionally sampled values, which are calculated as follows:

$$C_c = \frac{C}{I} \tag{13}$$

$$\overline{c_c^2} = \frac{\overline{c^2}}{I} - \frac{C^2(1-I)}{I^2} \tag{14}$$

and scaling factor, $A$, is given by:

$$A = \frac{2}{ERF\left(\frac{1-C_c}{\sqrt{2\overline{c_c^2}}}\right) - ERF\left(\frac{-C_c}{\sqrt{2\overline{c_c^2}}}\right)} \tag{15}$$

where $ERF()$ is the error function.

To calculate the flammability factor requires the integration of Equation (12) between the upper and lower flammability limits. Since the delta function only has finite amplitude at concentrations approaching zero (i.e. well below the LFL) the underbraced term in Equation (12) is effectively ignored. The remaining part is integrated as follows:

$$F = \frac{IA}{2}\left[ERF\left(\frac{c_U - C_c}{\sqrt{2\overline{c_c^2}}}\right) - ERF\left(\frac{c_L - C_c}{\sqrt{2\overline{c_c^2}}}\right)\right] \tag{16}$$

In deriving Equations (15) and (16), it is assumed that the mean and variance of the truncated Gaussian are equal to $C_c$ and $\overline{c_c^2}$. This was shown to provide a good approximation for the flammability factor model by Gant et al. (2011b).

To account for the presence of carbon dioxide in the gas mixtures, the upper and lower flammability limits ($c_U$ and $c_L$) are determined here using a modified version of Le Chatelier's law developed by Kondo et al. (2006):

$$c_L = \frac{\sum_i c_i}{\sum_i \frac{c_i}{L_i} - 0.01094 c_{co2}} \tag{17}$$

$$c_U = \left( \sum_i c_i \right) \left[ 100 - \frac{\left( \sum_i c_i n_i \right)}{B} \right] \tag{18}$$

where $B$ is given by:

$$B = \sum_i \frac{c_i n_i}{100 - U_i} + 0.00105 c_{CO2} + 0.00106 c_{CO2}^2 - 0.00106 c_{CO2}^3 \tag{19}$$

The concentrations of each of the flammable gases, $c_i$, have lower and upper flammable limits of $L_i$ and $U_i$ respectively, and $c_{CO2}$ is the concentration of carbon dioxide. In Equations (17) to (19), the parameters $c_i$, $L_i$, $U_i$ and $c_{CO2}$ are all expressed in terms of percentage by volume, i.e. the LFL of methane is included in the equations as $L_i = 5.0$, not 0.050. The parameter $n_i$ is the number of moles of oxygen consumed by one mole of fuel when the mixture is at the upper flammability limit. Assuming the combustion takes place in air, this is given by:

$$n_i = \frac{(100 / U_i) - 1}{1 + (79 / 21)} \tag{20}$$

# Tables

Table 1 Experimental Release Conditions

| **Volumetric Flow rate (l/min)** | 30 | 50 | 90 |
|---|---|---|---|
| **Exit velocity (m/s)** | 17.7 | 29.5 | 53.1 |
| **Reynolds number*** | 6453 | 10755 | 19359 |

*for 100% $CH_4$

Table 2 Ignition Response Classifications

| **Class** | **Ignition response** |
|---|---|
| 1 | No effect on pilot flame |
| 2 | Enhances combustion of pilot flame |
| 3 | Burns only in the presence of the pilot flame |
| 4 | Burns for a short period |
| 5 | Stable combustion, burns continuously |

Table 3 Flame front lift off distance and local velocity for pure methane

| **Release Velocity (m/s)** | **Lift Off Distance (cm)** | **Local Velocity (m/s)** |
|---|---|---|
| 29.5 | 6.91 | 8.77 |
| 53.1 | 12.84 | 9.64 |

# Figures

**(a)**

**(b)**

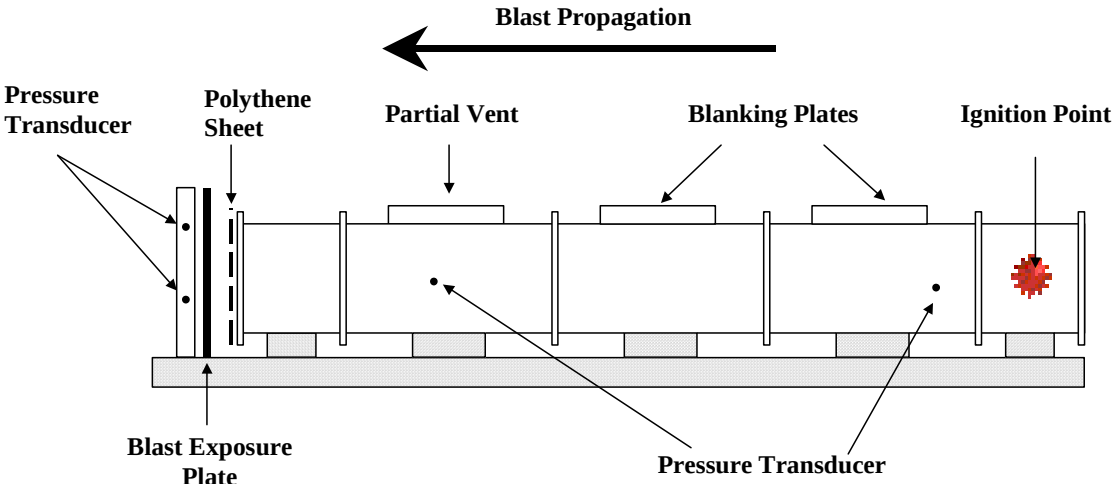


**(c)**

Figure 1 (a) Photograph of the 1.04 m diameter explosion vessel, (b) the ¾ open relief vent, and (c) a schematic of the apparatus

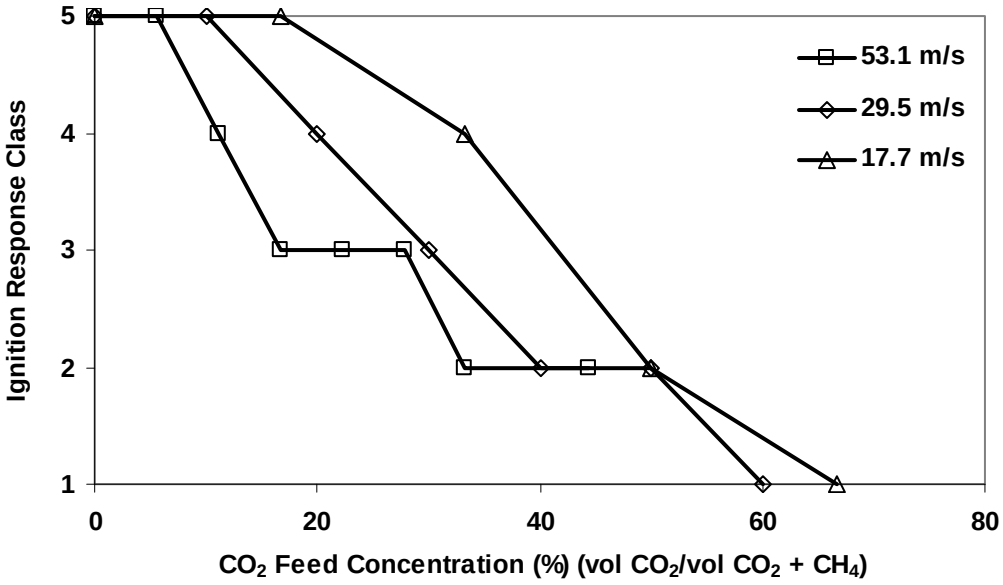


Figure 2 The change in ignition response class of gas mixtures with $CO_2$ feed concentrations over the range 0 – 70%, for exit gas velocities of 17.7 m/s, 29.5 m/s and 53.1 m/s.

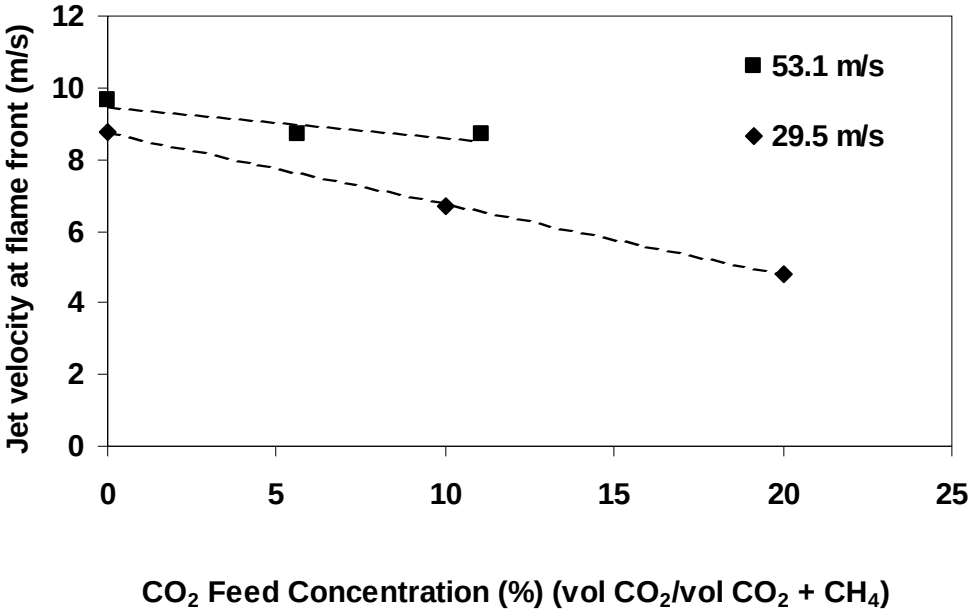


Figure 3 The effect of the $CO_2$ feed concentration on the local jet velocity at the flame lift off position for initial release velocities of 29.5 m/s (♦) and 53.1 m/s (■)

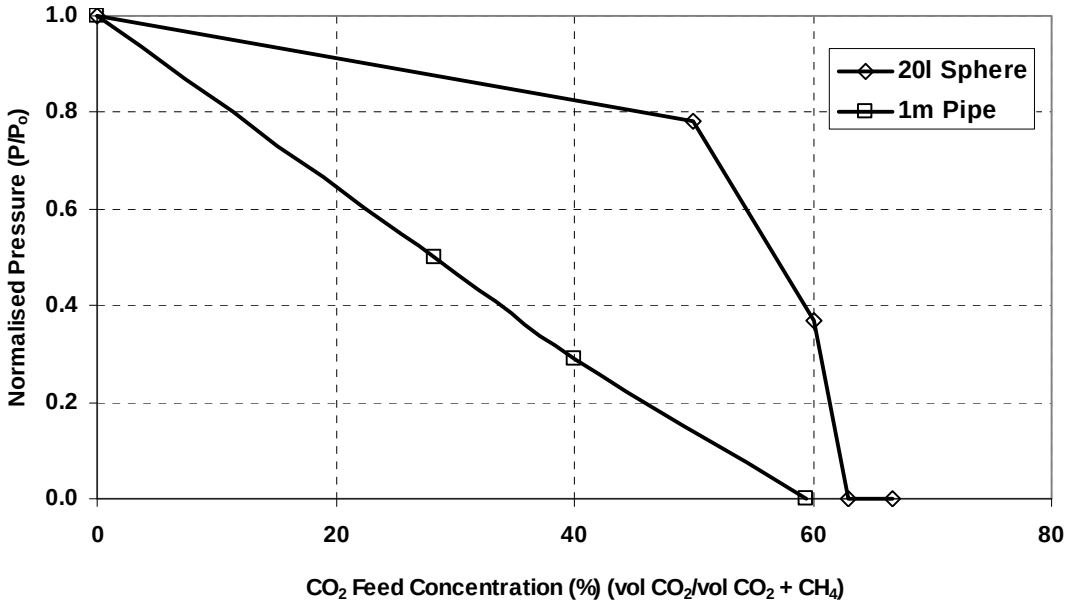


Figure 4 Maximum explosion overpressure for tests conducted in the 20 litre explosion sphere and the 1.04 m diameter pipeline. Pressure measurements are normalised against the maximum pressure, obtained without $CO_2$ present.

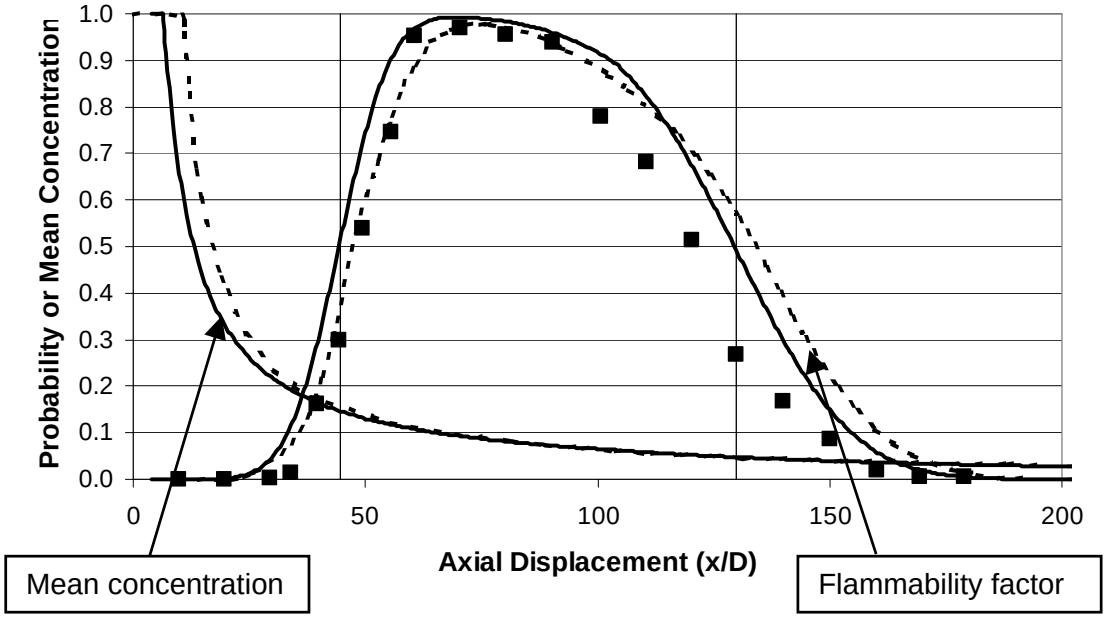


Figure 2 Comparison of flammability factor predictions and mean concentrations to ignition probability measurements for the natural gas jet studied by Smith et al. (1986); —: present model predictions; - -: previous prediction of Smith et al. (1986); ■ : measured ignition probability; vertical lines: mean UFL and LFL.

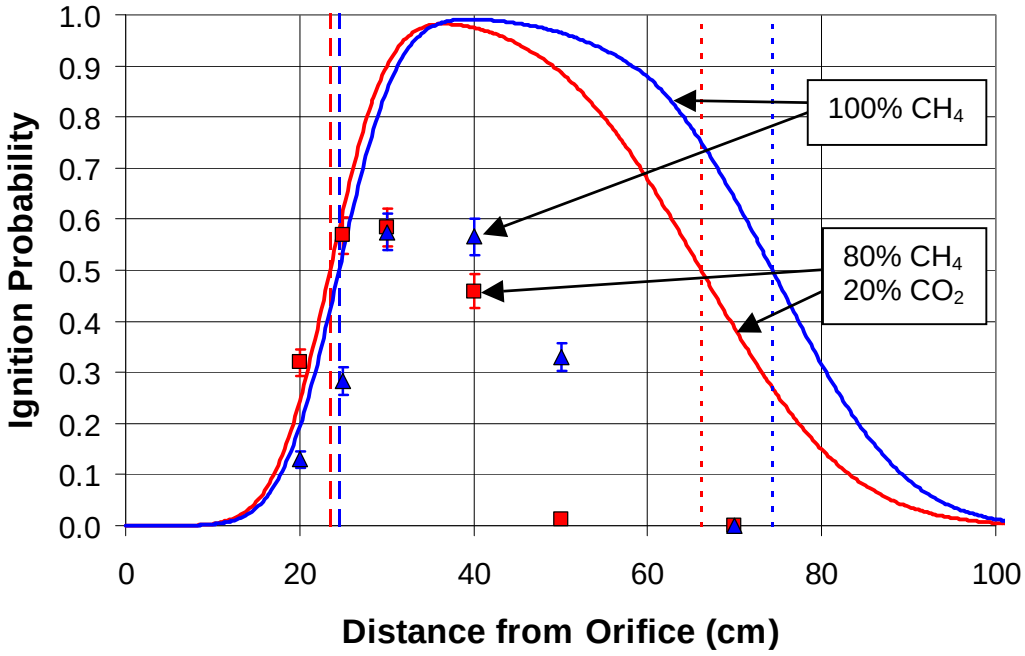


Figure 3 Measured ignition probability (symbols) and predicted flammability factor (solid lines) along the jet centreline. Vertical broken lines show LFL and UFL based on mean concentrations.

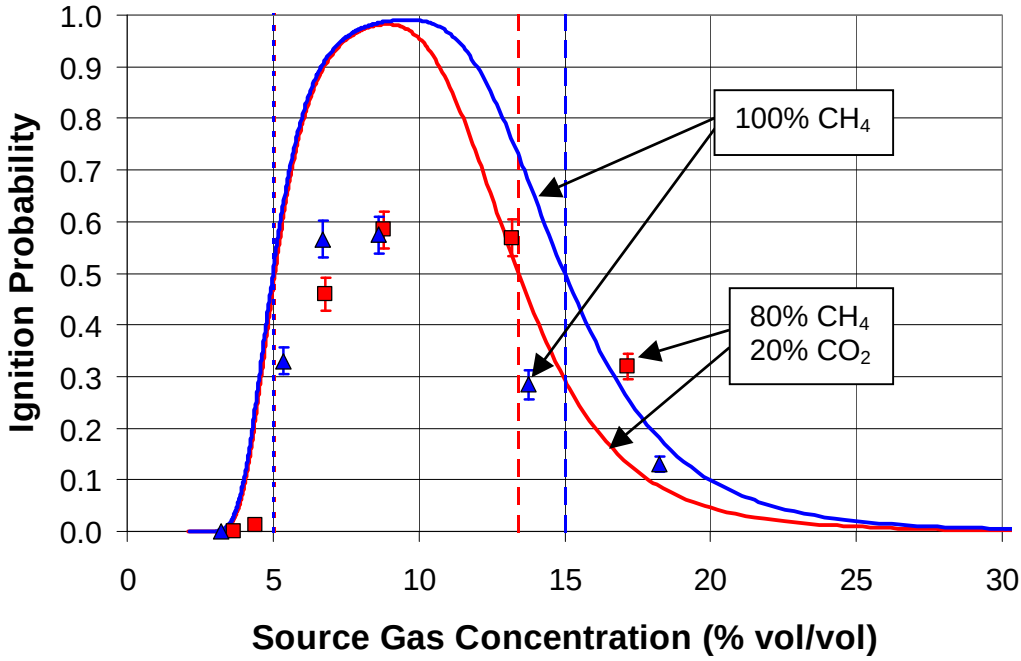


Figure 4 Measured ignition probability (symbols) and predicted flammability factor (solid lines) versus mean gas concentration along the jet centreline. Vertical broken lines show LFL and UFL based on mean concentrations.

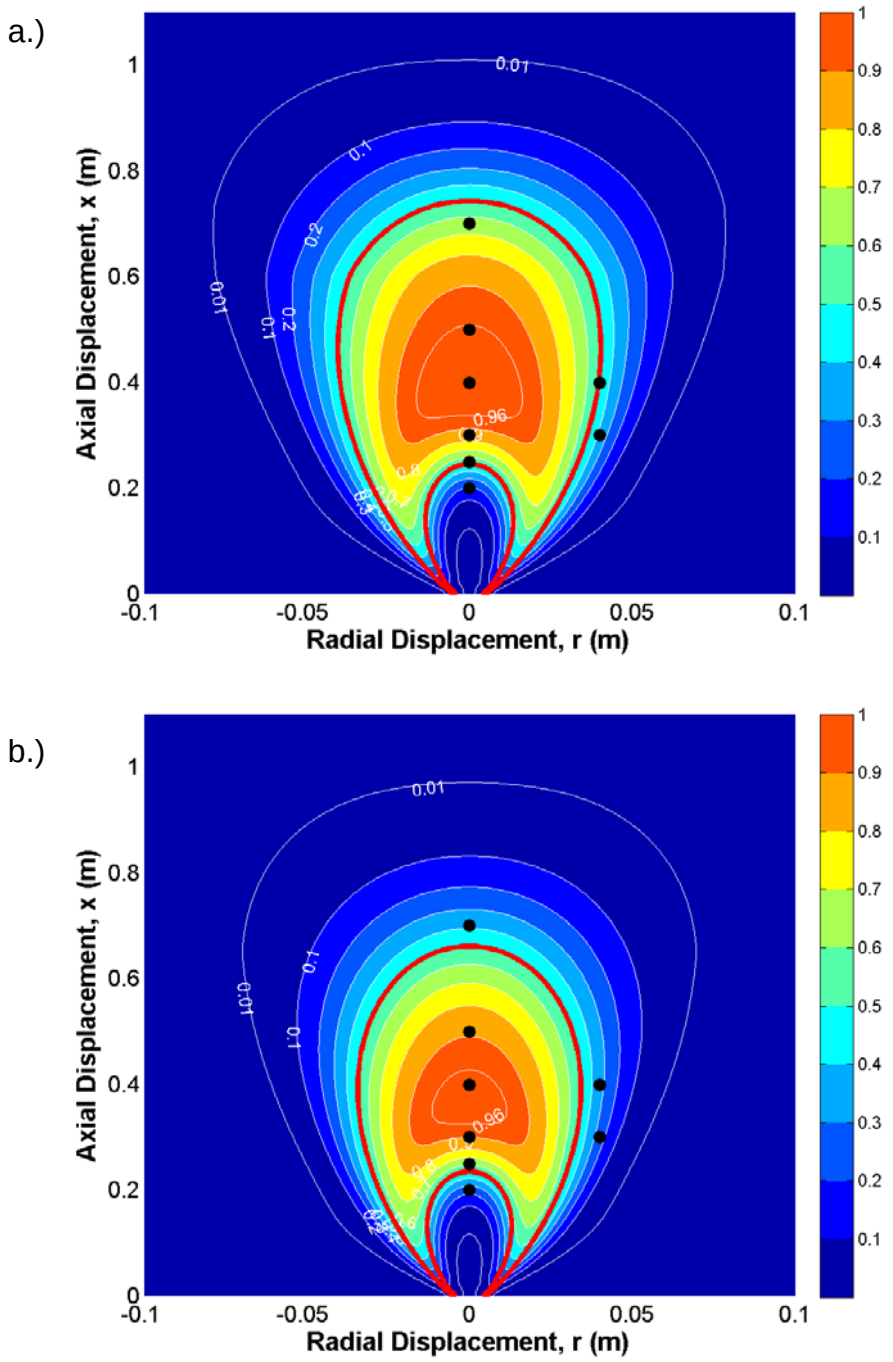


Figure 5 Predicted flammability factor for a.) pure methane; b.) 80% vol/vol methane, 20% vol/vol $CO_2$ mixture; —: mean UFL and LFL; ●: location of measurement positions.